Autosomal Dominant Hypophosphatemic Rickets Is Linked to Chromosome 12p13

Michael J. Econs,* Paul T. McEnery,‡ Felicia Lennon,* and Marcy C. Speer*
**Department of Medicine, Duke University Medical Center and the Durham Veterans Affairs Medical Center, Durham, North Carolina 27710; and ‡Department of Pediatrics, University of Cincinnati Medical Center and Cincinnati Children's Hospital, Cincinnati, Ohio 45229*

Abstract

Autosomal dominant hypophosphatemic rickets (ADHR) is an inherited disorder of isolated renal phosphate wasting, the pathogenesis of which is unknown. We performed a genome-wide linkage study in a large kindred to determine the chromosome location of the ADHR gene. Two-point LOD scores indicate that the gene is linked to the markers D12S314 [$Z(\hat{\theta}) = 3.15$ at $\theta = 0.0$], vWf [$Z(\hat{\theta}) = 5.32$ at $\theta = 0.0$], and CD4 [$Z(\hat{\theta}) = 3.53$ at $\theta = 0.0$]. Moreover, multilocus analysis indicates that the ADHR gene locus is located on chromosome 12p13 in the 18-cM interval between the flanking markers D12S100 and D12S397.

These data are the first to establish a chromosomal location for the ADHR locus and to provide a framework map to further localize the gene. Such studies will permit ultimate identification of the ADHR gene and provide further insight into phosphate homeostasis. (*J. Clin. Invest.* 1997. 100:2653–2657.) Key words: hypophosphatemia • rickets • osteomalacia • phosphate • chromosome 12

Introduction

Serum phosphate concentrations are regulated by a complex and poorly understood process. Insight into this process can be obtained by analysis of genetic aberrations in phosphate homeostasis. Autosomal dominant hypophosphatemic rickets (ADHR;[1] MIM 193100) is a disorder characterized by isolated renal phosphate wasting with inappropriately normal calcitriol concentrations. Patients frequently present with bone pain, rickets, and tooth abscesses. Recent studies (1) demonstrate that ADHR is incompletely penetrant, with variable expression and age of onset. Additionally, among those individuals who present during childhood, some individuals lose the phosphate wasting defect (1). The primary abnormality that underlies the disorder is unknown, and there are no animal models for the disorder. To elucidate the pathogenesis of this disorder, we performed a genome-wide linkage study in a large kindred to determine the chromosome location of the ADHR gene. Our results localize the disease gene to an 18-cM interval on the short arm of chromosome 12.

Methods

Patients. We obtained blood from 125 members of a North American Caucasian kindred (family 1406: 20 affected patients, 2 obligate carriers, 45 unaffected individuals, 40 individuals with unknown diagnostic status, and 18 spouses). The family has been described in detail previously (1). In brief, affected individuals were defined by the presence of hypophosphatemia, normocalcemia, and normal renal function. Serum phosphorus values for children were interpreted using age-specific normal ranges (2). In addition to serum biochemistries, histories, physical exams, and, in some instances, measurement of urinary phosphate excretion were used to determine phenotype. Individuals were classified as unknown with respect to diagnostic status if serum phosphorus values fell within the indeterminate range (2.4–3.1 mg/dl in adults), they gave histories of rickets or bowing as children that could not be documented, or other aspects of their presentation led to phenotypic uncertainty. Phenotypic variability in this disorder has been described previously (1). For all subjects, phenotype was determined with the clinician blinded to the individual's genotype. The study was approved by the Duke University Medical Center Institutional Review Board, and all subjects gave written informed consent before participating.

PCR amplification of microsatellite markers. DNA extraction from whole blood was performed as described previously (3). Primer pairs for the various microsatellite repeat markers were used to amplify 30 ng of genomic DNA. The PCR products were radiolabeled with ^{32}P by direct incorporation of [^{32}P]dCTP added to the reaction mixture or prior 5′ labeling of one of the primers using T4 polynucleotide kinase (4). The PCR products were separated by electrophoresis on standard polyacrylamide sequencing gels and visualized by autoradiography. Genotypes for key recombinant individuals were confirmed by resampling and regenotyping. Primer sequences for the markers are available from the Genome Database (http://gdbwww.gdb.org). Sequences for vWf primers are as follows: forward, 5′-CCCTAGTGGATGATAAGAATAATC and reverse, 5′-GGACAGATGATAAATACATAGGATGGATGG. All genetic marker data were maintained in the PEDIGENE database system (5).

Linkage analysis. Two-point and multipoint linkage analyses were performed using the VITESSE program (6). We assumed that the disease was transmitted as an autosomal dominant trait with disease allele frequency of 0.0001. Penetrance was modeled using two different approaches, a full-pedigree model and an affecteds-only model. For the full-pedigree model, we estimated the penetrance of the disease gene using maximum likelihood techniques as described by Chatkupt et al. (7). Specifically, the likelihood of the pedigree data

Presented in part at the annual scientific meetings of the Endocrine Society, in Minneapolis, MN on 11 June 1997, and the American Society of Human Genetics, 29 October through 1 November 1997.

Address correspondence to Michael J. Econs, M.D., Associate Professor of Medicine, Indiana University School of Medicine, 975 W. Walnut St., IB 445, Indianapolis, IN 46202. Phone: 317-274-7519; FAX: 317-278-0684; E-mail: mecons@iupui.edu

Received for publication 19 June 1997 and accepted in revised form 24 September 1997.

1. *Abbreviations used in this paper:* ADHR, autosomal dominant hypophosphatemic rickets; GNB3, guanine nucleotide–binding β3 polypeptide; HBD, hypophosphatemic bone disease; HYP, X-linked hypophosphatemic rickets; LOD, logarithm of the odds.

The Journal of Clinical Investigation
Volume 100, Number 11, December 1997, 2653–2657
http://www.jci.org

was maximized over disease allele penetrance. The maximum likelihood estimate of the penetrance in this pedigree was 0.57. We also used an affecteds-only or low-penetrance model, in which the penetrance of the disease allele was assumed to be low. This analysis uses genotypic data from all family members, but limits the use of phenotypic data to only those individuals affected with the disease. This conservative analysis allows inference of missing genotypes in family members unavailable for DNA sampling and maximizes the ability to establish linkage phase, while using the phenotypic data only from those individuals whose diagnostic status is certain. The approximate 95%-support interval for markers that generated a logarithm of odds (LOD) score > 3.0 was calculated using the one LOD score down method (8). Marker allele frequencies were calculated from a series of at least 80 unrelated Caucasian controls. These frequencies, along with more than 250 others, are available via the World Wide Web at http://www.medicine.duke.edu under the Section of Medical Genetics, or via anonymous ftp at dnadoc.mc.duke.edu in the /pub/ALLELE_FREQ directory.

Simulation studies were performed to assess the maximum attainable LOD score for the pedigree using the computer program SIMLINK (9). For these analyses, we assumed the availability of a tetraallelic marker with frequencies 0.40, 0.30, 0.20, and 0.10, generating a heterozygosity value of 0.70, which was linked to the ADHR locus at 5% recombination.

The genetic map for the ADHR region was developed using CEPH (10) pedigree genotype data extracted from the Cooperative Human Linkage Center database (http://www.chlc.org). The CRIMAP program was used as described previously (11) to determine the most likely order of and sex-averaged distances between those markers that were in the region of the ADHR locus, were most informative in the pedigree, and were determined by visual inspection of the pedigree data to flank the disease locus. These markers included D12S100, D12S314, vWf, CD4, D12S397, and D12S77.

Results

We undertook a genome-wide linkage search with microsatellite repeat markers spaced at 20–30-cM intervals. We analyzed > 170 markers across the genome. LOD scores > 3 (corresponding to odds of linkage $> 1{,}000{:}1$) were obtained only for markers on chromosome 12p. Two-point LOD scores and the associated maximum likelihood estimate of the recombination fraction (θ) between the ADHR gene locus and the markers are listed in Table I. In the full-pedigree analysis, several markers yielded LOD scores > 3.0, including D12S314, vWf, and CD4, which produced LOD scores of 3.15, 5.32, and 3.53, respectively, at $\theta = 0.00$. Each of these markers yielded higher LOD scores for the affecteds-only analysis (4.11, 5.65, and 3.73, respectively).

For the multipoint analysis, we generated a genetic map, with sex-averaged recombination fractions as follows: tel-D12S100 - 0.08 - D12S314 - 0.04 -vWf - 0.03 - CD4 - 0.03 - D12S397- 0.06-D12S77-cen. The order of the markers in this genetic map was supported with odds of 1,000:1 over the next most likely map order.

Multipoint linkage analysis using the full-pedigree model yielded a multipoint LOD score of 8.14, when the ADHR gene was placed at no recombination with vWf (Fig. 1). For the affecteds-only analysis, the maximum multipoint LOD score was 8.13, also at no recombination with vWf. For comparison, the simulation results determined that the maximum overall LOD score attainable from this pedigree is 9.94 for the full-pedigree analysis and 7.63 for the affecteds-only analysis (at a genetic distance of 5 cM). Since the multipoint LOD scores were highest at markers that demonstrated no recombination with the ADHR gene, we repeated the simulation studies to determine the highest potential LOD score assuming no recombination between the disease and marker locus. At zero recombination, the maximum attainable LOD scores were 10.76 and 8.38 for the full-pedigree and affecteds-only analyses, respectively, indicating that virtually all of the available linkage information in the pedigree was extracted in the multipoint analysis.

Visual inspection of the genetic marker data showed the distal flanking genetic marker to be D12S100 and the proximal flanking marker to be D12S397, spanning an approximate distance of 18 cM. Fig. 2 illustrates a portion of family 1406 demonstrating segregation of a disease-associated haplotype, a proximal recombinant event with D12S397, and recombination events establishing D12S100 as the distal flanking marker.

Discussion

The investigation of families in which diseases altering phosphate homeostasis are segregating provides an invaluable tool for elucidating the genetic control of these mechanisms. Linkage analysis is the first step in identifying a gene by the positional cloning approach. The advantage of this approach, which has been used to identify a large number of genes (12), is that knowledge of gene function is not necessary to locate the disease gene. In this study, we localized the ADHR gene locus segregating in this family to an 18-cM interval flanked

Table I. Two-Point LOD Scores for Markers Surrounding the ADHR Locus

Marker	Full-pedigree analysis							Affecteds-only	
	θ	θ	θ	θ	$Z(\hat{\theta})$	$\hat{\theta}$	*95%-support interval*	$Z(\hat{\theta})$	$\hat{\theta}$
	0.00	0.05	0.10	0.15					
D12S100	−10.49	−0.65	0.40	0.82	0.99	0.23	NA	0.88	0.24
D12S314	3.15	2.87	2.58	2.26	3.15	0.00	0.00–0.18	4.11	0.00
vWf	5.32	4.87	4.39	3.87	5.32	0.00	0.00–0.11	5.65	0.00
CD4	3.53	3.33	3.03	2.68	3.53	0.00	0.00–0.15	3.73	0.00
D12S397	−3.57	2.04	2.13	1.96	2.13	0.09	NA	1.96	0.09
D12S77	−0.67	4.21	4.17	3.87	4.25	0.07	0.05–0.16	4.17	0.07

Two-point LOD scores for chromosome 12 markers versus ADHR for full-pedigree (penetrance = 0.57) and affecteds-only analyses. θ, Recombination fraction. $\hat{\theta}$, recombination fraction at the maximum LOD score. $Z(\hat{\theta})$, maximum LOD, *NA*, Not applicable.

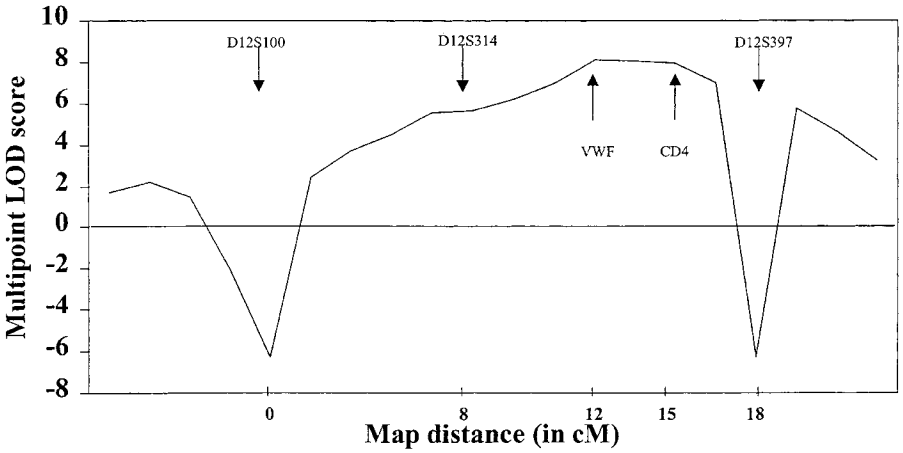

Figure 1. Multipoint LOD score analysis for ADHR. Multilocus analysis of the ADHR locus demonstrates that the most likely location for the gene is at no recombination with vWf. The analysis was limited to the map region spanning from D12S100 to D12S397 due to computational constraints.

distally by D12S100 and proximally by D12S397. This conclusion is supported by both the full-pedigree and affecteds-only analyses, which yielded LOD scores significantly greater than the classic threshold of 3.0. Interestingly, affecteds-only analysis yielded higher two-point LOD scores than full-pedigree analysis, suggesting that some of the pedigree members currently classified as unaffected may be gene carriers. This result is consistent with our previous data, which demonstrated that the disease is not highly penetrant (1).

Before localization of the ADHR gene in this family, we assessed three genes that were feasible candidates based on their function and potential pathogenetic relationship to ADHR. These candidates included two sodium-dependent phosphate cotransporters (located on chromosomes 6p and 5q35) and stanniocalcin (8p21). Stanniocalcin was a feasible candidate for ADHR, following recent observations (13, 14) indicating that parenteral administration of human stanniocalcin results in increased uptake of phosphorus in the mammalian kidney.

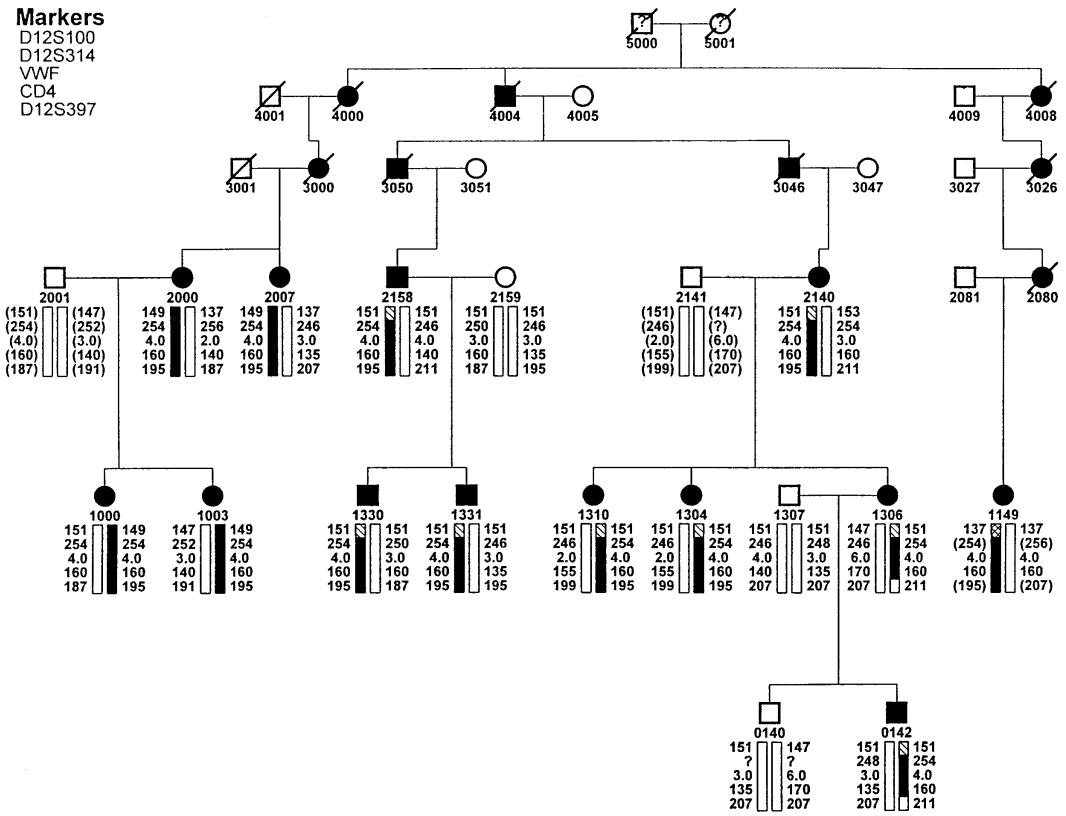

Figure 2. Pedigree showing evidence for segregation of haplotype with ADHR disease phenotype. *Filled bars* and *symbols*, Affected individuals. *Open bars* and *symbols*, Unaffected individuals. *Circles*, Females. *Squares*, Males. Genetic marker genotypes are listed under individuals. Note that this pedigree also demonstrates evidence for recombination between the ADHR gene and D12S397 in transmission from individual 2140 to individual 1306, thus defining the proximal boundary for the minimum candidate region. Two linkage-phase unknown recombination events define D12S100 as the distal flanking marker (i.e., in the pedigree, the disease gene segregates with the 149, 137, and 151 alleles). The linkage phase of results in parentheses is inferred based on most likely haplotype. Results for individuals 2001 and 2141 are inferred but not genotyped. *NT*, Not tested.

In all cases, markers surrounding these regions generated consistently negative LOD scores.

With the identification of the 18-cM candidate interval on 12p13, a directed investigation of candidate genes located in this region is now feasible. A computer search of the Online Mendelian Inheritance in Man database (OMIM) (http://www3.ncbi.nlm.nih.gov:80/Omim) identified many known genes on 12p13. These include several members of the proline-rich protein family (15), microfibril-associated glycoprotein 2 (16), neuron-specific enolase (17), and guanine nucleotide–binding β3 polypeptide (GNB3; reference 18). GNB3 is part of a 223-kb gene–rich contig which contains several genes of known function, including CD4, ubiquitin isopeptidase T, and triosephosphate isomerase, as well as several genes of unknown function, including "gene A," "gene B," and Destrin-2 (19, 20). None of the above genes are obvious candidates for the ADHR gene, with the exception of GNB3 and "gene A." GNB3 codes for the β3 G protein subunit (18), and one of the splice variants of "gene A" contains seven putative transmembrane domains consistent with membership in the G protein–coupled receptor superfamily (19). In light of the role that G proteins and G protein–coupled receptors play in transmembrane hormonal and sensory transduction processes, it is tempting to speculate that a mutation, either activating or inactivating, in GNB3 or "gene A" might result in phosphate wasting.

Our study capitalized on the availability of a single large pedigree. This approach allowed us to localize the ADHR gene without concerns about genetic heterogeneity; however, it limits the generalizability of our results. Whether the gene on 12p is responsible for all cases of ADHR remains to be determined. Furthermore, it will be of interest if studies of hypophosphatemic bone disease (HBD; reference 21) demonstrate linkage to 12p13, since this disorder may be a forme fruste of ADHR. Studies linking HBD to 12p13 would support the notion that ADHR and HBD are not separate disorders. Additionally, linkage studies of tumoral calcinosis, an autosomal dominant disorder (22) characterized by increased phosphate retention and elevated calcitriol concentrations (the converse of ADHR), should examine the 12p13 region, since tumoral calcinosis and ADHR could result from a different mutation in the same gene.

Regulation of phosphate homeostasis is a poorly understood process, and perturbation of any one of a number of steps in this process could lead to phosphate wasting. Current models of phosphate homeostasis indicate that renal phosphate wasting could result from (*a*) mutations in a gene that enable the organism to assess extracellular phosphate concentrations (a phosphate sensor); (*b*) activating mutations in a gene(s) that codes for a renal phosphate-wasting hormone (phosphatonin) or its receptor (including associated G proteins); (*c*) mutations in a gene(s) that codes for a phosphate-conserving hormone or its receptor; (*d*) mutations in genes that code for repressors or inducers for the above hormones; (*e*) mutations in genes that code for enzymes that activate or degrade these hormones; and (*f*) mutations in genes that code for the sodium-dependent phosphate cotransporters. The primary defect in ADHR results in isolated renal phosphate wasting, and the disorder could result from any of the previously mentioned mechanisms. Isolation of the ADHR gene may result in identifying one of the genes in the above model or, if the ADHR gene codes for a protein that has none of the above functions, isolation of the ADHR gene may result in changes to the current model. Indeed, such a situation existed with the gene responsible for X-linked hypophosphatemic rickets (HYP). HYP is an X-linked dominant disorder that results in isolated phosphate wasting. Positional cloning efforts led to the identification and cloning of the gene responsible for HYP, now referred to as PEX (23). PEX is a member of the M13 metalloprotease family. Although the function of this protein in phosphate homeostasis has not yet been determined, it likely functions to degrade a phosphate-wasting hormone (phosphatonin) or to activate a phosphate-conserving hormone. Since previous models failed to postulate an enzymatic role for the HYP gene product, the identification of PEX resulted in modifications to models of phosphate homeostasis. Similarly, identification of the ADHR gene may lead to additional changes in models of phosphate homeostasis.

In summary, our data are the first to establish a chromosomal location for the ADHR gene and to provide a framework for further localization of the gene. Identification of the ADHR gene will require a multifaceted approach, including assessment of candidate genes and investigation of other ADHR families, which may provide additional recombinants to narrow the interval of interest on chromosome 12p13. Such studies will permit ultimate identification of the ADHR gene and provide important insight into phosphate homeostasis.

Acknowledgments

This work was supported by grants AR-42228, AR-27032, M01-RR-30, M01-RR-08084, and NS-26630, from the National Institutes of Health.

References

1. Econs, M.J., and P.T. McEnery. 1997. Autosomal dominant hypophosphatemic rickets/osteomalacia: clinical characterization of a novel renal phosphate wasting disorder. *J. Clin. Endocrinol. Metab.* 82:674–681.

2. Greenberg, B.G., R.G. Winters, and J.B. Graham. 1960. The normal range of serum inorganic phosphorus and its utility as a discriminant in the diagnosis in congenital hypophosphatemia. *J. Clin. Endocrinol. Metab.* 20:364–379.

3. Econs, M.J., D.F. Barker, M.C. Speer, M.A. Pericak-Vance, P.R. Fain, and M.K. Drezner. 1992. Multilocus mapping of the X-linked hypophosphatemic rickets gene. *J. Clin. Endocrinol. Metab.* 75:201–206.

4. Sambrook, J., E.F. Fritsch, and T. Maniatis. 1989. Molecular Cloning: A Laboratory Manual, second ed. Cold Spring Harbor Laboratory, Cold Spring Harbor, NY.

5. Haynes, C.S., M.C. Speer, M. Peedin, A.D. Roses, J.L. Haines, J.M. Vance, and M.A. Pericak-Vance. 1995. PEDIGENE: a comprehensive data management system to facilitate efficient and rapid disease gene mapping. *Am. J. Hum. Genet.* 57:A193.

6. O'Connell, J.R., and D.E. Weeks. 1995. The VITESSE algorithm for rapid exact multilocus linkage analysis data via genotype set-recoding and fuzzy inheritance. *Nat. Genet.* 11:402–408.

7. Chatkupt, S., M.C. Speer, Y. Ding, M. Thomas, E.S. Stenroos, J.J. Dermody, M.R. Koenigsberger, J. Ott, and W.G. Johnson. 1994. Linkage analysis of a candidate locus (HLA) in autosomal dominant sacral defect with anterior meningocele. *Am. J. Med. Genet.* 52:1–4.

8. Conneally, P.M., J.H. Edwards, K.K. Kidd, J.M. Lalouel, N.E. Morton, J. Ott, and R. White. 1985. Report of the Committee on Methods of Linkage Analysis and Reporting. *Cytogenet. Cell Genet.* 40:356–359.

9. Ploughman, L.M., and M. Boehnke. 1989. Estimating the power of a proposed linkage study for a complex genetic trait. *Am. J. Hum. Genet.* 44:543–551.

10. Dausset, J., H. Cann, D. Cohen, M. Lathrop, J.M. Lalouel, and R. White. 1990. Centre d'etude du polymorphisme humain (CEPH): collaborative genetic mapping of the human genome. *Genomics.* 6:575–577.

11. Straub, R.E., M.C. Speer, Y. Luo, K. Rojas, J. Overhauser, J. Ott, and T.C. Gilliam. 1993. A microsatellite genetic linkage map of human chromosome 18. *Genomics.* 15:48–56.

12. Collins, F.S. 1995. Positional cloning moves from perditional to traditional. *Nat. Genet.* 9:347–350.

13. Olsen, H.S., M.A. Cepeda, Q.Q. Zhang, C.A. Rosen, B.L. Vozzolo, and

G.F. Wagner. 1996. Human stanniocalcin: a possible hormonal regulator of mineral metabolism. *Proc. Natl. Acad. Sci. USA*. 93:1792–1796.

14. Wagner, G.F., B.L. Vozzolo, E. Jaworski, M. Haddad, R.L. Kline, H.S. Olsen, C.A. Rosen, M.B. Davidson, and J.L. Renfro. 1997. Human stanniocalcin inhibits renal phosphate excretion in the rat. *J. Bone Miner. Res.* 12:165–177.

15. Azen, E.A., and N. Maeda. 1988. Molecular genetics of human salivary proteins and their polymorphisms. *Adv. Hum. Genet.* 17:141–199.

16. Gibson, M.A., G. Hatzinikolas, J.S. Kumaratilake, L.B. Sandberg, J.K. Nicholl, G.R. Sutherland, and E.G. Cleary. 1996. Further characterization of proteins associated with elastic fiber microfibrils including the molecular cloning of MAGP-2 (MP25). *J. Biol. Chem.* 271:1096–1103.

17. Oliva, D., L. Cali, S. Feo, and A. Giallongo. 1991. Complete structure of the human gene encoding neuron-specific enolase. *Genomics.* 10:157–165.

18. Levine, M.A., P.M. Smallwood, P.T. Moen, Jr., L.J. Helman, and T.G. Ahn. 1990. Molecular cloning of beta 3 subunit, a third form of the G protein beta-subunit polypeptide. *Proc. Natl. Acad. Sci. USA*. 87:2329–2333.

19. Ansari-Lari, M.A., D.M. Muzny, J. Lu, F. Lu, C.E. Lilley, S. Spanos, T. Malley, and R.A. Gibbs. 1996. A gene-rich cluster between the CD4 and triosephosphate isomerase genes at human chromosome 12p13. *Genome Res.* 6:314–326.

20. Ansari-Lari, M.A., Y. Shen, D.M. Muzny, W. Lee, and R.A. Gibbs. 1997. Large-scale sequencing in human chromosome 12p13: experimental and computational gene structure determination. *Genome Res.* 7:268–280.

21. Scriver, C.R., W. MacDonald, T. Reade, F.H. Glorieux, and B. Nogrady. 1977. Hypophosphatemic norachitic bone disease: an entity distinct from X-linked hypophosphatemia in the renal defect, bone involvement, and inheritance. *Am. J. Med. Genet.* 1:101–117.

22. Lyles, K.W., E.J. Burkes, G.J. Ellis, K.J. Lucas, E.A. Dolan, and M.K. Drezner. 1985. Genetic transmission of tumoral calcinosis: autosomal dominant with variable clinical expressivity. *J. Clin. Endocrinol. Metab.* 60:1093–1096.

23. 1995. A gene (PEX) with homologies to endopeptidases is mutated in patients with X-linked hypophosphatemic rickets. The HYP Consortium. *Nat. Genet.* 11:130–136.